Front. Optoelectron.
DOI 10.1007/s12200-017-0724-6

REVIEW ARTICLE

Research and developments of laser assisted methods for translation into clinical application

Ronald SROKA (✉)[1,2], Nikolas DOMINIK[1,2], Max EISEL[1,2], Anna ESIPOVA[3], Christian FREYMÜLLER[1,2], Christian HECKL[1,2], Georg HENNIG[1,2], Christian HOMANN[1,2], Nicolas HOEHNE[1,2], Robert KAMMERER[2,5], Thomas KELLERER[1,2], Alexander LANG[1,2], Niklas MARKWARDT[1,2], Heike POHLA[2,4], Thomas PONGRATZ[1,2], Claus-Georg SCHMEDT[1,3], Herbert STEPP[1,2], Stephan STRÖBL[1,2], Keerthanan ULAGANATHAN[1,2], Wolfgang ZIMMERMANN[2,4], Adrian RUEHM[1,2]

1 Laser-Forschungslabor, LIFE-Center, Hospital of University, Ludwig-Maximilians University Munich, Munich, Germany
2 Department of Urology, Hospital of University, Ludwig-Maximilians University Munich, Munich, Germany
3 Department of Vascular Surgery, Diakonie Klinikum, Schwäbisch Hall, Germany
4 Labor für Tumorimmunologie, LIFE-Center, Hospital of University, Ludwig-Maximilians University Munich, Munich, Germany
5 Friedrich-Loeffler-Institute, Federal Research Institute for Animal Health, Greifswald- Insel Riems, Germany

Abstract Biophotonics and laser medicine are very dynamic and continuously increasing fields ecologically as well as economically. Direct communication with medical doctors is necessary to identify specific requests and unmet needs. Information on innovative, new or renewed techniques is necessary to design medical devices for introduction into clinical application and finally to become established after positive clinical trials as well as medical approval. The long-term endurance in developing light based innovative clinical concepts and devices are described based on the Munich experience. Fluorescence technologies for laboratory medicine to improve non-invasive diagnosis or for online monitoring are described according with new approaches in improving photodynamic therapeutic aspects related to immunology. Regarding clinically related thermal laser applications, the introduction of new laser wavelengths and laser parameters showed potential in the treatment of varicose veins as well as in lithotripsy. Such directly linked research and development are possible when researchers and medical doctors perform their daily work in immediate vicinity, thus have the possibility to share their ideas in meetings by day.

Keywords translational biophotonics, thermal laser application, fluorescence diagnosis, on-line monitoring, lithotripsy, phlebology, photodynamic therapy (PDT), laboratory medicine

Received April 5, 2017; accepted May 22, 2017

E-mail: Ronald.Sroka@med.lmu.de

1 Introduction

Biophotonics and laser medicine is a broad research and development area to meet challenges in clinical diagnostics and therapy as well as health care issues by means of advanced optical technologies. People working in this field are highly motivated by their vision of improving clinical therapeutic procedures or to extend into new fields for lasers in medicine. Novel biomedical laser applications and new types of lasers widen the possible spectrum of laser-tissue interactions to improve target-oriented, precise application of laser radiation in clinical practice.

Highly sophisticated targeting strategies including endogenous or applied fluorophores pave the way for new diagnosis and treatment modalities. Synergistic approaches of photodynamic therapy and immune-modulatory effects are new fields for research and clinical studies. Theoretical considerations and modeling of laser light distribution in tissue with subsequent energy transfer and light-tissue interactions constitute a solid basis for therapy planning in patients, particularly if combined with improved light delivery and monitoring techniques.

Although there are a variety of potential examples in diverse medical societies in which laser assisted applications are part of routine diagnostics and therapy, here the Munich experience and activities are summarized, some of which are at the entrance into clinical routine. It is intended to describe the way of insufficiently solved or unsolved problems in clinical medicine which can be overcome by suitable technical solutions, thus to identify the "white spots" as well as to bridge the gap between research bench and bed side.

2 Non-invasive screening method to diagnose iron deficiency

Iron deficiency affects more individuals than any other health problem, especially children, women of child-bearing age and pregnant women, both in developed and developing countries. At present, detection of iron deficiency requires obtaining a blood sample and subsequent laboratory analysis, limiting the availability of screening in resource-limited settings.

Zinc protoporphyrin (ZnPP) is a molecule formed in the last step of heme synthesis, where normally a ferrous ion is inserted into a Protoporphyrin IX molecule, forming heme ("Iron Protoporphyrin"). If the availability of iron is low, a divalent zinc ion is inserted instead, forming ZnPP. Therefore, a reduced availability of iron leads to an increased level of ZnPP production. ZnPP is bound to hemoglobin and remains within the erythrocytes during their lifetime as a marker for iron deficiency. Even for patients with severe iron deficiency, only traces of ZnPP are found within the erythrocytes, which make the detection cumbersome.

Here a method is described based on fiber probe fluorescence spectroscopy on the lower lip to non-invasively measure the erythrocyte ZnPP/heme ratio as an established indicator of iron deficiency, without the need for taking a blood sample.

To optically measure the ZnPP/heme ratio, the fluorescence of ZnPP is excited at 425 nm and its characteristic fluorescence emission is detected by a spectrometer in a wavelength range between about 500 and 750 nm. As the ZnPP is closely bound to heme, which is strongly absorbing at 425 nm, it can be shown that the intensity of the fluorescence emission is proportional to the ratio of the concentrations of ZnPP/heme for a wide range of erythrocyte concentrations [1]. In blood and even more in tissue, other fluorophores are present that are also excited in the blue wavelength region and have overlapping emission spectra with ZnPP [2,3]. In tissue, this leads to a perturbing fluorescence signal about 100 times stronger than the fluorescence emission of ZnPP.

This fluorescence background can be largely eliminated by acquiring a second fluorescence spectrum with excitation at 407 nm and subsequent subtraction from the first spectrum. At 407 nm, most perturbing fluorophores are excited similarly in comparison to 425 nm excitation. ZnPP, however, is only excited with a reduced efficiency of around 0.22. Consequently, the fluorescence background is reduced by about 93% in the difference spectrum, and the contribution of ZnPP fluorescence can be extracted by spectral fitting.

For the measurement on a subject, a fused silica glass fiber with a diameter of 1 mm and embedded in a 12 mm stainless steel ferrule was placed on the red vermillion of the lower lip as shown in Fig. 1. The 407 nm excitation light was switched on by a foot switch and tissue fluorescence spectra were continuously acquired. A spectral fitting algorithm determined 'on-the-fly' the amount of blood absorption found around 576 nm, the 'blood absorption index'. It has been shown [3] that for sufficiently high blood absorption indices, the measured ZnPP fluorescence intensity correlates well with the ZnPP/heme ratio in blood. Consequently, the device indicated sites on the lower lip to the examiner by a green light, when

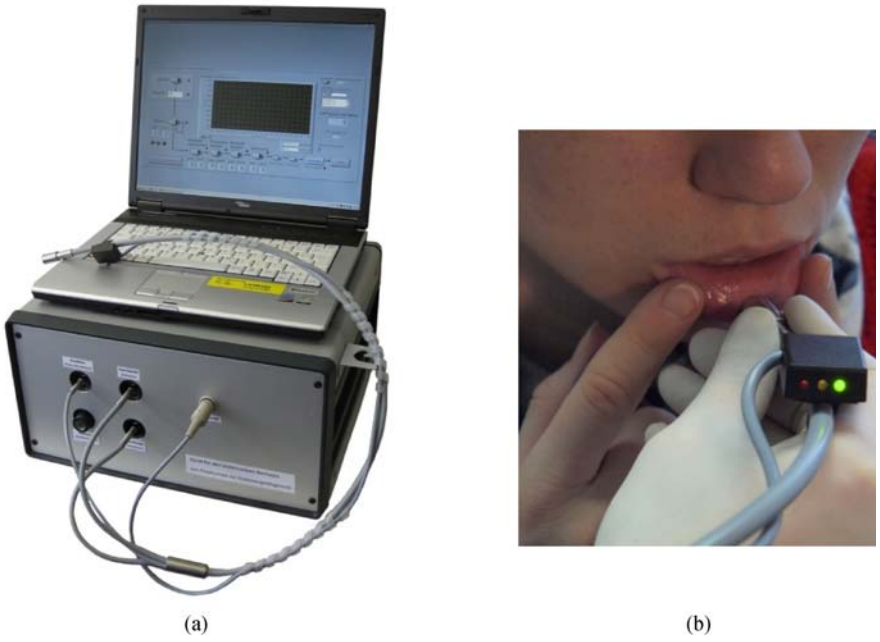

(a) (b)

Fig. 1 Prototype ZnPP fluorometer device is shown (a), with the optical fiber attached to the front side. The applicator tip is brought in contact of the lower lip of a patient (b), while the feedback light indicates a measurement site suitable for a reliable ZnPP measurement

the blood absorption index exceeded 7×10^{-3}. When such a site was found, the examiner initiated the measurement by pressing the foot switch again. A series of fluorescence spectra was acquired with alternating excitation at 425 nm and at 407 nm. After calculating the difference spectra from two associated spectra, the ZnPP fluorescence was determined by a spectral fitting algorithm that relies on minimizing the second derivative of the residual.

A clinical study on 56 women after childbirth was conducted. In addition to the non-invasive measurements, ZnPP was determined from an ethylenediaminetetracetic acid (EDTA) blood sample for each subject. The non-invasive measurement results were compared with a reference high-performance liquid chromatography (HPLC) determination of ZnPP. In Fig. 2, the non-invasively determined ZnPP fluorescence (scaled) is compared with the reference ZnPP determination on blood of the same subjects. The normal range is 20 to 40 µmol ZnPP/mol heme, values above 50 µmol ZnPP/mol heme are clearly elevated. For a threshold value of 50 µmol ZnPP/mol heme, the sensitivity and specificity of the non-invasive determination compared with the reference was 97% and 90%, respectively. The limits of agreement (1.96 × the robust standard deviation) of the non-invasive method against the reference HPLC determination were 19 µmol ZnPP/mol heme (95% confidence interval: 14 to 24 µmol ZnPP/mol heme). For comparison, the limits of agreement of the HPLC method in two determinations on the same set of samples were 16 µmol ZnPP/mol heme (95% confidence interval: 13 to 19 µmol ZnPP/mol heme).

These results establish proof-of-concept for the fluorescence spectroscopic determination of ZnPP non-invasively at the lower lip. Due to the similar limits of agreement of the non-invasive method and the HPLC reference, these methods seem to be virtually exchangeable. The non-invasive method combines several advantages: An established marker for iron deficiency (ZnPP) can be measured reliably and rapidly at the point of care, while no blood drawing and subsequent laboratory processing is required. These advantages allow for a broader iron deficiency screening in populations where a blood drawing is rarely done, for example in children, and/or where laboratory equipment is unavailable, for example in developing countries. The proposed non-invasive method to detect erythrocyte ZnPP bares the potential to revolutionize iron deficiency screening.

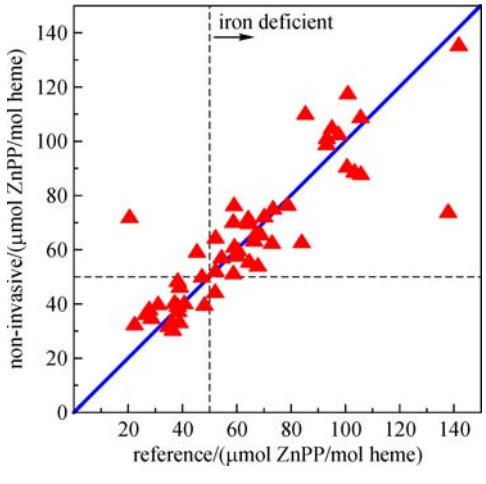

Fig. 2 Results of a clinical study on 56 women after childbirth. Shown is the comparison of the non-invasive ZnPP fluorescence measurements with the reference HPLC determination

3 Investigation for point of care screening for acute porphyria

Acute porphyria is a rare genetic disease of the heme synthesis with latent and acute phases [4]. During an acute attack, heme precursors such as porphyrins and porphobilinogen accumulate in the body and are excreted via urine [4,5]. Due to the ambiguous symptoms ranging from abdominal pain and rashes to neurological symptoms and tetraparesis [4,6], the disease is often overlooked [6]. In the United States, the diagnosis is delayed by 15 years on average [6]. This can be mostly attributed to a severe lack of reliable and cost efficient screening tests [6], which makes it impossible to screen extensively for acute porphyria.

A screening test which is based on a dual-wavelength-excitation fluorescence measurement on urine for the quantification of porphyrins in urine which differentiates uroporphyrin from coproporphyrin is under investigation. Since the differentiation of uroporphyrin and coproporphyrin offers information required for the differentiation of acute porphyrias [7], this method offers higher specificity for screening for acute porphyria compared to screening for total urinary porphyrins. Urinary porphyins can be increased in urine due to high coproporphyrin as in several diseases linked to porphyrinuria [6].

The method used was similar to a method on blood plasma [8]. Urine samples of healthy subjects were spiked with uroporphyrin and coproporphyrin (all from Sigma Aldrich, St. Louis, Missouri, USA) in physiologically relevant concentrations, mixed with 50 µL HCl 1 M[1)] per mL urine, put into glass cuvettes (C4012-465, Thermo Fisher Scientific, Waltham, Massachusetts, USA) and illuminated with a 397 nm and a 409 nm laser diode (SLD3134VR-31, Laser Components GmbH, Olching, Deutschland) with equal power for fluorescence measurements. The concentration of porphyrin stock solutions was determined by absorption spectroscopy using extinction coefficients [9]. Spectra were collected using a spectrometer (S2000, Ocean Optics, Dunedin, FL, USA). Optical

1) 1 M = 1 mol

fibers (FT030, Thorlabs, Newton, New Jersey, USA) were used for light guiding from the light sources to the sample and from the sample to the spectrometer. The device was controlled and data evaluation was performed by home-made software.

In Fig. 3, a comparison between excitation spectra of uroporphyrin and coproporphyrin (UP I and CP I, respectively) in urine at pH 7 and pH 1.5 are shown. In the acidic regime, the excitation spectra shift apart from each other and are much narrower, leading to a high ratio between the excitation spectra of uroporphyrin and coproporphyrin. This can be used to selectively excite either uroporphyrin at 409 nm or coproporphyrin at 397 nm.

In Fig. 4, the spectra of a urine sample spiked with uroporphyrin and coproporphyrin derived from dual wavelength excitation are shown (Fig. 4(a)). In Fig. 4(b), calibration curves are shown which describe the relation of fluorescence intensity of each porphyrin in urine with the

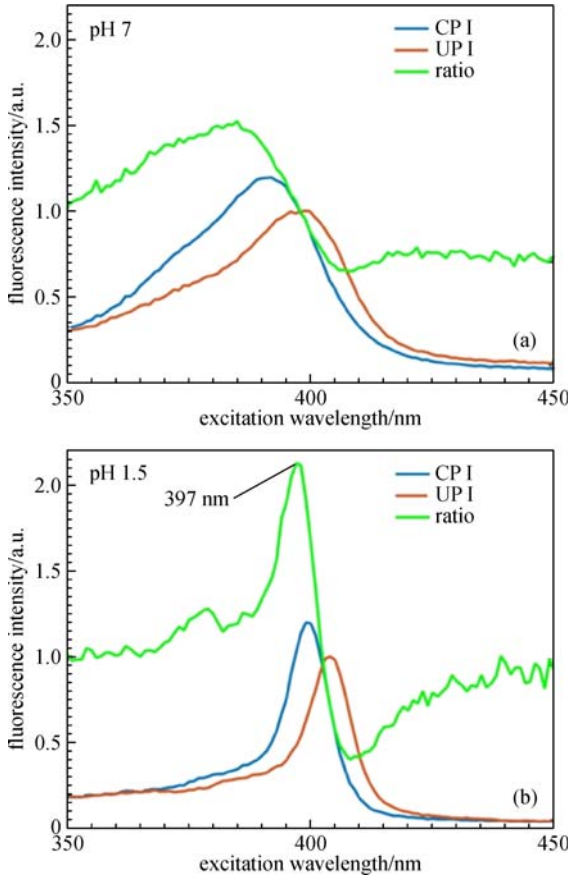

Fig. 3 Fluorescence excitation of coproporphyrin I and uroporphyrin I spectrum at (a) pH = 7 and (b) pH = 1.5 at the same molar concentration. The quotient of coproporphyrin to uroporphyrin excitation spectra reveals the ideal excitation wavelength for selective excitation of either porphyrin (green). For the acidic samples, the ratio yields a much higher difference between uroporphyrin and coproporphyrin excitation, which allows for a more precise differentiation between the two porphyrins

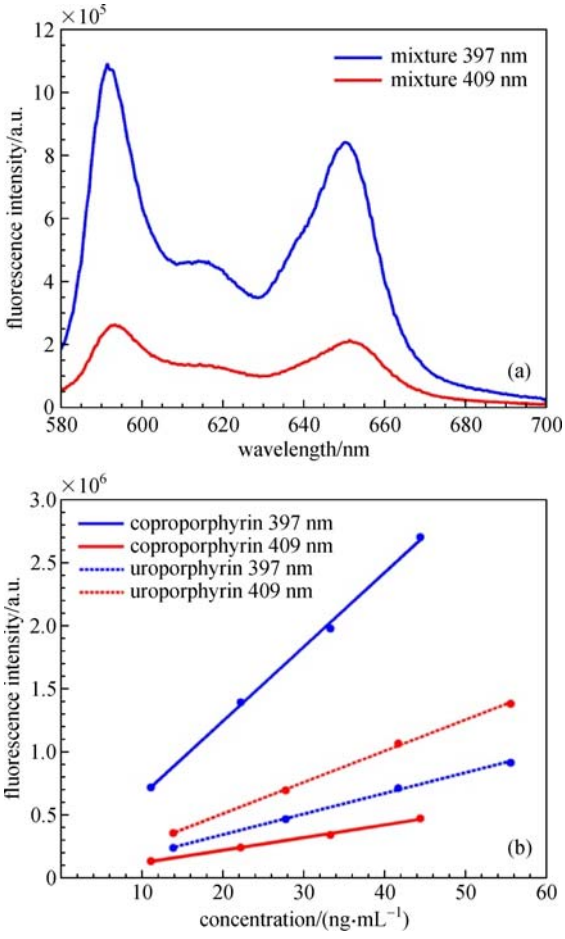

Fig. 4 Fluorescence spectra of urine spiked with uroporphyrin and coproporphyrin (a). The picture shows, that 397 nm excitation yields a much higher fluorescence than 409 nm excitation, which is indicative of a sample with a higher amount of coproporphyrin than uroporphyrin. From the calibration curves (b), two equations for each excitation wavelength can be derived. With the intensity measured during the two wavelength excitation, the equations can be solved and return the concentration of each porphyrin

porphyrin concentration. The equations describing the fluorescence intensity-concentration correlation can be combined to two equations, one for each wavelength, with two unknowns, one for each concentration. Those equations can be solved using the fluorescence intensity measured on an unknown sample.

The results show that uroporphyrin and coproporphyrin can be distinguished using dual wavelength excitation at 397 and 409 nm. The quantification of each porphyrin concentration is possible. This is the first step towards a routine point of care testing method required for the general screening of patients with unresolved abdominal pain. The method, however, does not fully oxidize possibly present porphyrinogens, which are not fluorescent, but count toward the total urinary porphyrins [10]. Porphobilinogen, the most specific marker for acute porphyria, which shows no fluorescence cannot be quantified using a

straight forward point of care approach. Therefore essential further research is needed to find a way for its simple optical detection.

4 Optical spectroscopy to enhance accuracy and safety of stereotactic biopsy

A self-manufactured fiber-based device for stereotactic brain tumor biopsies is developed. 5 aminolevulinic acid (5-ALA)-induced protoporphyrin IX (PpIX) fluorescence is used to localize vital tumor tissue [11]; the spectral analysis of polychromatic light diffusely transmitted through the investigated tissue between two fiber tips serves to detect blood vessels [12] and thus helps to minimize the risk of inducing cerebral hemorrhages. For both tasks, ray tracing simulations and experiments on phantoms mimicking the optical properties of brain tumor tissue [13,14] were performed.

First, the sensitivity of PpIX-based tumor detection was investigated for two different excitation wavelengths (405 and 633 nm; corresponding to absorption maxima of PpIX [11]) on optical phantoms. The effect of blood interference was studied by placing artificial blood layers of 10 – 400 µm thickness between fiber and phantom.

It was found that 405-nm-excitation shows a 50-fold higher sensitivity, but physiologic PpIX concentrations of a few µM [15] should be well detectable with both wavelengths. In addition, 633-nm-excitation is considerably superior in case of blood-covered tumor tissue. For instance, a 50 µm blood layer blocks the 405-nm-excited fluorescence completely, but reduces the 633-nm-excited signal by less than 50% [11]. Additionally, using 633 nm as PpIX excitation wavelength is more suitable for PpIX-assisted detection of high-grade gliomas in stereotactic biopsy due to its higher penetration depth with respect to blood and human tissue. Thus, a better congruence between mechanically sampled (usually a few mm^3) and optically probed volume can be achieved. The potentials of the red excitation in presence of blood are not only interesting for the stereotactic biopsy procedure, but also for other applications such as photodynamic therapy or fluorescence-guided resection.

Second, blood vessel detection with a two-fiber probe (inter-fiber distance: 1.8 mm, see Fig. 5(a)) was experimentally tested by using a blood-filled glass capillary as blood vessel dummy, which was submerged into the tumor-mimicking phantom [13,14], and simulated via ray tracing. The remitted light was analyzed at two wavelengths with strongly differing hemoglobin absorption (578 and 650 nm) [16]. For this analysis, the ratio of remitted light intensities $R = I_{578}/I_{650}$ was calculated. Blood absorbs strongly at 578 nm, but quite weakly at 650 nm. This causes a convergence of R to 0 in presence of blood vessels in immediate vicinity of the fiber probe.

Depending on their orientation, blood vessels are detectable up to 800 – 1200 µm ahead of the probe on the basis of a considerably reduced remission ratio I_{578}/I_{650} as compared to the background value. The possibility of detecting a blood vessel is demonstrated in Fig. 5.

The sensitivity of the blood vessel detection strongly depends on position and orientation of the blood vessel relative to the two side-view fibers (not shown here). The differentiation between blood vessels and blood in the interstitium leaking from an injured minor blood vessel in the vicinity of the biopsy site remains an issue of the technique in the presented form. The described method was successfully tested with a real biopsy needle probe on

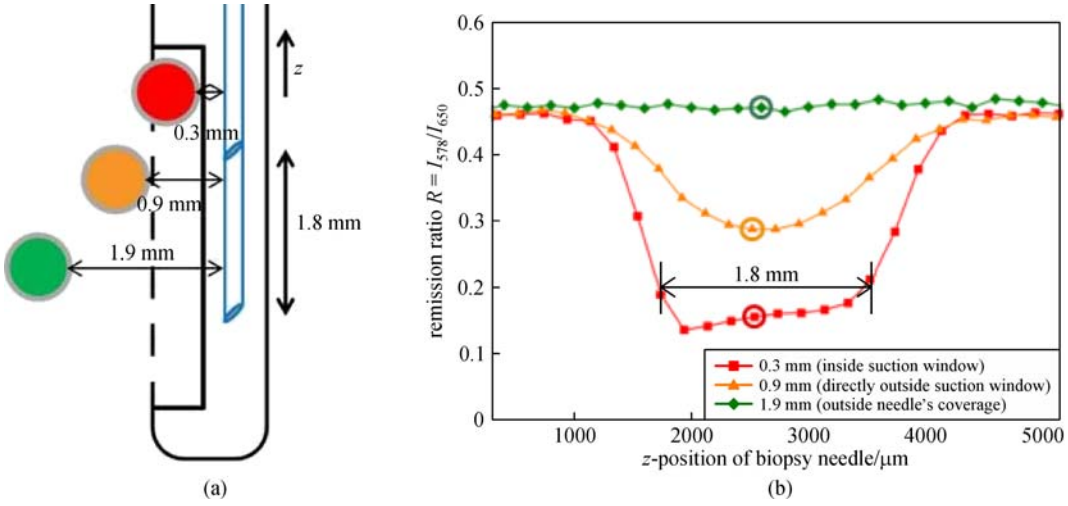

Fig. 5 (a) Schematic of a central phantom experiment: The opto-mechanical biopsy needle (here: only with side-view fibers) was immerged in a liquid brain phantom at different distances from a blood-filled glass capillary (drawn in red, orange and green, respectively). After adjusting the fiber-to-capillary distance, the needle was moved in z-direction. The capillary orientation was perpendicular to the drawing plane. (b) Experimental results of the remission ratio I_{578}/I_{650} for the three fiber-to-capillary distances indicated left

both optical phantoms and *ex-vivo* porcine brain tissue, thus showing potential to improve the safety of stereotactic biopsy and offering a simple and readily realizable alternative to existing concepts regarding blood vessel detection. It appears to have a high clinical potential similar to laser-Doppler-flowmetry [17].

Finally, a biopsy needle capable of detecting brain tumors and blood vessels was realized. Two side-view fibers are needed for such a biopsy needle. Side-view fibers are optical fibers beveled at an angle of 45° on the front and metal-coated with aluminum via vapor deposition or sputtering. The two side-view fibers are positioned and fixed in a biopsy needle by means of biocompatible glue as in Fig. 6. With a suitable optical setup and these two fibers, it is possible to detect tumor tissue and blood vessels within the suction window of the biopsy needle. In addition, a plane fiber is added to detect tumor tissue in front of the needle.

This biopsy needle was already tested *ex-vivo* on optical phantoms and porcine brain tissue. Due to the fixed integration of the fibers into the biopsy needle, the fiber probe does not have to be removed from the biopsy channel for tissue sampling, which benefits the clinical workflow and assures a maximal congruence of optically and mechanically sampled volumes. The possibility of sterilization and thus a multiple use of such a biopsy needle remains an issue of investigation.

5 Interstitial Photodynamic Therapy (iPDT)

Interstitial photodynamic therapy (iPDT), based on the photosensitizer PpIX which is selectively enriched in tumor cells after administration of the pre-drug 5-ALA, is proposed to treat bulky tumor tissue in its original location, which could be an entire solid tumor or a non-resectable portion thereof. PDT in this case involves selective accumulation of the photosensitizer PpIX in tumor cells, the absorption of light by the PpIX molecules, the transfer of the excitation energy to intracellular oxygen resulting in the generation of reactive oxygen species (ROS), and finally the destruction of the affected tumor cells via necrosis or apoptosis. The light is delivered to the tumor cells via optical fibers introduced into the solid tumor [18], along especially carefully planned trajectories as sketched in Fig. 7 [19]. For interstitial light application, the optical fibers exhibit cylindrical diffuser regions near the distal fiber tip. Light entering the diffuser region from the optical fiber is scattered into the tissue. The further light propagation within the tissue is determined by the morphology of the tissue. In the simplest approximation, the tissue can be described by population-averaged and spatially homogeneous optical properties, i.e., index of refraction (n), absorption (μ_a) and reduced scattering coefficient (μ_s'). Dosimetry can then be performed for several light diffusers with known positions on the basis of the diffusion approximation [20]. The goal of the light dosimetry planning is to ensure a sufficient light dose in each region of the tumor volume, where the latter has previously been demarcated during treatment planning [21]. The entire treatment planning procedure must also ensure that side effects such as overheating or blood vessel perforation are ruled out [11,12,21].

The light diffusers distributing the treatment light into the tissue can also be utilized to collect scattered treatment light as well as fluorescence light from the illuminated tumor volume and guide it outward through the corresponding optical fiber [21]. This way, each of the fibers can temporarily be used additionally for signal detection during the described spectral online monitoring. If all other fibers are illuminated during signal collection, a gross signal is obtained that, e.g., allows to monitor photobleaching of the photosensitizer during treatment. More detailed information can be obtained from the signal measurement if treatment light is applied through only one of the light diffusers, while all others are turned off. In this case, transmission and fluorescence characteristics can be gathered from different tumor regions, depending on the pair of light diffusers used for tumor illumination and signal detection in each case.

In the case of cylindrical light diffusers, the detected signal is generated by light emission from a cylindrical

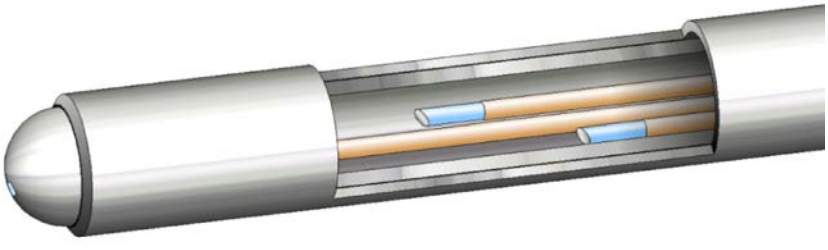

Fig. 6 Sketch of an opto-mechanical biopsy needle with three integrated glass fibers for light delivery and collection. One bare-end fiber is used to detect tumor tissue via PpIX fluorescence in front of the needle. Two side-view fibers are placed inside the tissue suction window to assess the sucked tissue regarding the presence of tumor tissue (via PpIX fluorescence) and blood vessels (via remission spectrometry)

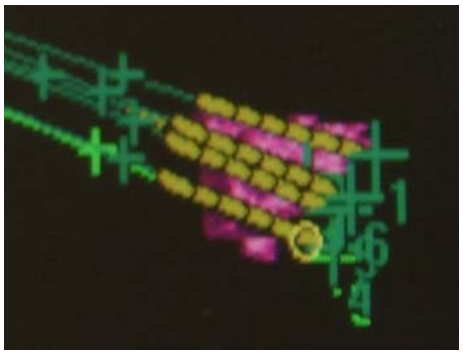

Fig. 7 Schematic representation of interstitially placed light applicators in the treatment planning software. The active portions along the stereotactic trajectories from which radiation emanates are indicated in yellow, the tumor volume to be irradiated is indicated in purple [19]

surface, transportation of the light through the tissue toward a second cylindrical light diffuser, whose cylindrical surface acts as a collection/detection device. The detailed characteristics of light emission and detection depend on the particular light diffusers. As a general approximation concept, both diffuser regions may be represented by an infinitely thin linear source and detector, respectively. While this concept neglects many details of the actual scenario, it is still helpful to detect problematic situations in a particular tumor region. For this purpose, the relative positioning of the two diffuser regions must be taken into account properly. This can be done in a very simplified approach by substituting the linear diffuser sections by a number of equidistant point sources and summing over all source/detection point pairs. More refined models will involve detailed Monte Carlo simulations.

6 Gene chip analysis uncovers the upregulation of immune modifiers by sublethal photodynamic therapy (PDT)

In addition to immediate phototoxic cell destruction, photodynamic therapy (PDT) is known to induce an immune response [22–25]. Compared to other forms of cancer treatment, the PDT-induced immunogenic cell death (ICD) is considerably more potent in this regard and was even proposed to be exploited for the production of antitumor vaccines [26–28].

In the context of aminolevulinic acid (5-ALA) mediated PDT for the treatment of malignant brain tumors, especially glioblastoma multiforme (GBM), the observed incidence of long-term survivors [18,21,29–31] may at least partly be due to the induction of a competent immune response. The hypothesis is that tumor cells, which undergo sublethal PDT, overexpress and excrete damage associated molecular patterns (DAMP), which in turn lead to attraction and maturation of immune cells, finally killing tumor cells, which had survived the phototoxic damage during PDT irradiation.

To investigate the possible roles of a modified gene expression in sublethally treated tumor cells by 5-ALA mediated PDT, the transcriptomes before and after low-dose PDT were compared using gene chip analysis [32]. Human glioblastoma cell lines U87 and U373 were grown in 6-well plates in Roswell Park Memorial Institute (RPMI)-1640 medium with 5% fetal calf serum and incubated with 5-ALA at a concentration of 50 μg/mL for 16 h and irradiated with 635 nm laser light with different light doses. Cell viability after PDT was determined with the CellTiterBlue test and apoptosis with the Apo-ONE test (both Promega). PDT treated cells were harvested after 4 or 24 h and RNA was isolated. 1 – 5 μg of RNA was amplified, labeled with biotin and hybridized to Affymetrics Gene Chip U133 Plus 2.0 oligonucleotide microarrays. For the identification of expression changes between sample groups, the Chip software was used, for identification of pathways with significantly changed expression between sample groups the Gene Set Enrichment Analysis (GSEA 2.0, MIT) software.

Both glioma cell lines tested showed a light dose dependent damage and could be completely killed with sufficiently high light doses (Fig. 8). The induction of apoptosis as measured by activation of caspase 3/7 was highest at light doses, where cell viability was reduced to about 50%. As cell damage leading to apoptosis is likely to be associated with multiple changes in the transcriptome, light doses leading to maximum apoptosis were used in experiments to identify, which genes are significantly up- or down-regulated.

Among the most upregulated genes, heat shock proteins, early response genes, immune modifiers and anti-proliferative factors were dominating as shown in Fig. 9. Down-regulation of genes was found less frequently. These genes encode for often cell growth and survival promoting proteins (data not shown). Among the genes highly upregulated were a number of immune response genes, such as the chemokine genes CXCL2 and CXCL3 and the cytokine gene IL6. The associated proteins are potent immune modifiers. Strong upregulation was also found for some genes encoding for heat shock proteins, where HSPA6 (HSP70) may be the most relevant one (red arrows in Fig. 9). It could be shown that HSP70 induces dendritic cell activation in human glioblastoma spheroids [33]. Interestingly, HSP70 upregulation was a lot more prominent with 5-ALA mediated sublethal PDT than it was when the photosensitizer Photofrin® was used under identical conditions (data provided in Ref. [32]).

Taken together, these results suggest that non-lethal PDT induces anti-tumor immune responses and, therefore, supports the hypothesis that 5-ALA based PDT of GBM may be a suitable therapy, even if a complete eradication of all tumor cells by phototoxicity alone is not guaranteed.

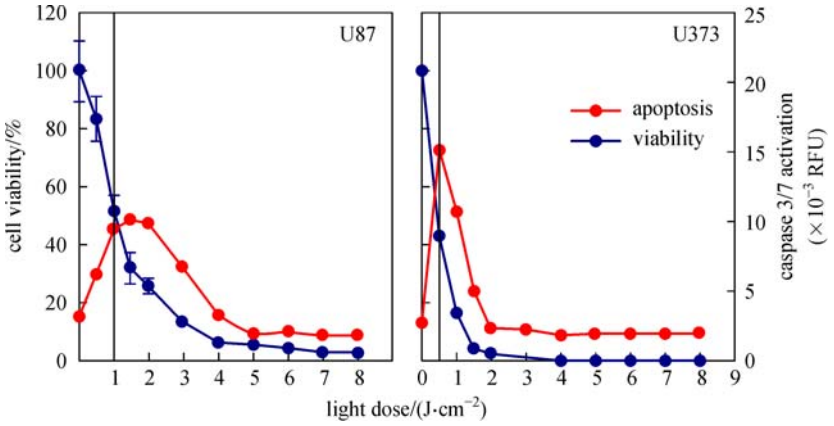

Fig. 8 Light dose dependent survival and caspase 3/7 activation of U87 and U373 cells. For investigation of the transcriptome, sublethal light doses of 1 J/cm^2 (U87) and 0.5 J/cm^2 (U373) were applied (black lines in the graphs). Adopted from Ref. [32]

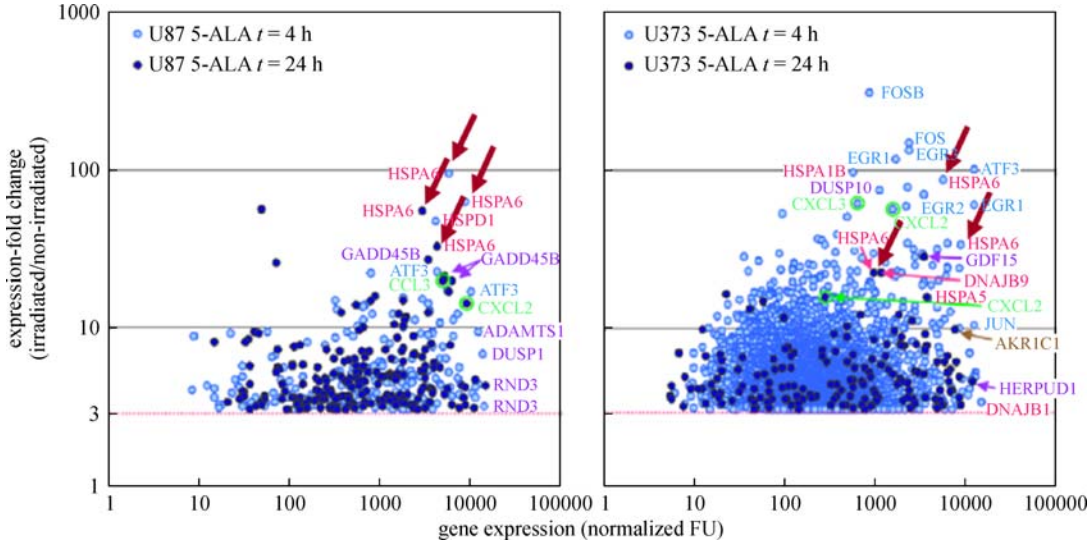

Fig. 9 Genes upregulated by non-lethal PDT. Adopted from Ref. [32]

7 Endoluminal laser treatment of varicose veins

Varicose veins are widened vessels due to weakened connective tissue and insufficiency of vein valves. Located on the lower extremities, the symptoms are subjectively described by individual sensations like heavy legs, tension, swelling, pain while standing and sitting, discoloring, phlebitis. The involved structures are mainly the vena saphena magna and the vena saphena parva. In half of the cases, patients need surgical intervention with the main goal of complete destruction of the affected vessel. Besides methods of conservative surgery and stripping treatments, during the past 15 years endoluminal procedures like sclero-therapy, radio-frequency ablation and endovenous laser therapy (ELT) have gained attention among the medical community. First clinical results of ELT were published in the beginning of this millennium [34,35]. Due to the diversity of laser parameters (e.g., wavelength, light application system, power, irradiance, irradiation) and the corresponding variable interaction with the target tissue, physicians requested for a precise, reproducible, safe, standardized procedure and treatment protocol which includes the strategic investigation of light application systems as well as potential online feedback. Thus the endoluminal application of laser energy implies the necessity of controlling a variety of parameters all together influencing the alteration produced on the vein wall. Variations in the laser wavelength, power settings and irradiance result in different temperature levels and thermal alterations up to perforation [36–38].

The first approach was the development of a specific radial emitting fiber to deliver the energy in direction to the vessel wall [39–42], which are now commercially available. Technologies such as the 360° radial fiber (models of 1-ring as well as 2-ring are in use) in combination with

1470 nm laser light [39] look promising to induce safe, reliable and reproducible tissue alteration for ELT.

Nowadays, further improvements were shown experimentally by using lasers emitting at 1940nm (Vela XL, Boston Scientific) in continuous mode. This IR-wavelength is highly absorbed by water molecules compared to other wavelength used for ELT so far. Until 2013, this wavelength was used only in urology and by ear, nose and throat surgeons.

In a single-center, prospective observational study, patients with saphenous reflux were treated with the 1940 nm laser in combination with radial fiber emission (1-ring) and continuous pullback under general, spinal or only tumescent anesthesia. The procedure was performed by means of ultrasound guidance, simultaneous miniphlebectomy was performed in all cases.

Clinical evaluations were performed preoperatively and postoperatively after three days, four weeks, six months and 12 months. The treated veins showed a progressive reduction in the diameter over the period of one year (e.g., mean reduction of the diameter of greater and small saphenous veins postoperatively at one year was 40% and 56%, respectively ($p < 0.05$)). In a few patients at one year follow-up, the treated vein could not be delineated and completely or partly disappeared. The mean linear endovenous energy density (LEED) applied was 59.2 J/cm for the greater and 47.3 J/cm for the small saphenous veins, respectively. Complete occlusion of the treated saphenous vein was defined as absence of flow on color Doppler imaging and could be achieved in 97.7% patients at 12 months. Partial occlusion was observed and was defined as reflux more than 3 cm distal to the junction. The complication rates observed were less than or comparable to the other endothermal and surgical procedures. In the early postoperative phase, paraesthesia was the most common complication in 8.5% patients which could be associated with high energy applied. In 2.3% cases ecchymosis related to the tumescence anesthesia and not with the laser energy directly were documented. There were neither reported skin burns nor phlebitis and no patients reported pain.

It can be summarized that endovenous laser therapy using a thulium laser with radial fiber emission efficiently eliminates the reflux in the saphenous veins via occlusion and achieves significant diameter reduction with no reflux recurrence at one-year follow-up. These benefits are offered with low postoperative pain and analgesia requirement.

Based on the reduction of undesirable side effects and the accelerated convalescence, endovenous treatment methods became the treatment option of first choice for insufficient veins in some countries [43,44]. Despite such improvements, some minor effects like carbonization and adhesion of the fiber to the vessels wall could be still observed during the clinical procedure. Therefore implementation of feedback-technologies like temperature monitoring may further assist standardization of the procedure.

8 Fiber-based temperature measurement using ruby fluorescence

In medical laser application like ELT, knowing the temperature in the treated area is of advantage. Metal or semiconductor based temperature sensors are strongly affected by the preferred wavelength favored for such treatments, similar effects occur when used in an magnetic resonance (MR) scanner. It is thereby preferable to have a temperature measurement system at hand that is less sensitive to thermal laser radiation. Optical thermal sensors can provide those properties [45,46]. Based on the method of analyzing the temperature-dependent spectral fluorescence intensity [47] a temperature measurement system was constructed.

An optical set-up was designed for excitation of the ruby by a frequency doubled diode-pumped solid-state (DPSS) Nd:YAG laser, which is coupled into the measurement fiber. The fiber probes consist of 400 μm multimode fibers with a ruby sphere of 1 mm diameter attached to the distal end as shown in Fig. 10. The back-guided fluorescence light of the ruby crystal is separated from the excitation with a dichroitic mirror and coupled into a fiber leading to a spectrometer for spectral analysis.

Computation of the temperature of the ruby attached to the fiber tip is performed by means of preliminarily generated characteristic curves. For the generation of the characteristic curves, the ruby fluorescence spectrum is divided into three areas: the *R* line at 694 nm and two broadband emissions to the higher and lower wavelength sides of the *R* line, respectively. Different numbers of spectra were acquired per measurement to reduce the statistical noise, considerations were made between accuracy and the time required for one measurement. For determination of the accuracy, a characteristic curve was created. Thereafter the fiber was heated in a stirred water bath again. The calculated ruby temperature and the water temperature were recorded during heating and cooling, meanwhile the number of averaged spectra was varied. The difference of the calculated ruby temperature and the reference temperature was used to determine the accuracy of the measurement. Investigations regarding the influence of thermal laser irradiating the ruby sphere showed that improvements can be achieved up to an accuracy better than ± 1.5°C with averaging of spectra but resulting also in prolongation of the measurement time.

Finally, a temperature measuring system based on the analysis of the temperature dependent fluorescence of a ruby crystal could be developed [48]. This sensor can be manufactured to being inert and biocompatible. It was tested to be useable within a high electro-magnetic field such as a laser light irradiation field. Clinically adapted

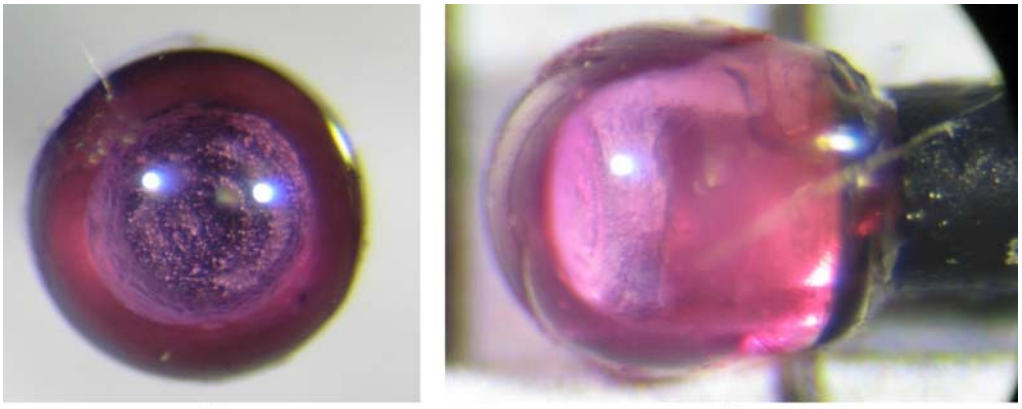

Fig. 10 Temperature sensor consisting of ruby sphere (outer diamter, OD = 1 mm) attached to an optical fiber (core diameter 400 μm). (a) Front view; (b) side view

ex-vivo experiments in a blood filled vein showed accurate measurements when the sensor tip is positioned in the vein parallel to and directly within the radially emitting therapeutic fiber [48].

Different approaches exist for measuring temperature with an optical fiber, e.g., fiber Bragg gratings and fluorescence lifetime. Each has its advantages and shortcomings, so considerations have to be made what method suits best to the requirements, or if combinations of different methods are possible and of advantage. With a temperature measurement system that is little affected by thermal laser radiation, temperature can be monitored online during treatment, with higher patient safety as consequence. Eventually the integration of an optical temperature measurement system into the treatment fiber is possible.

9 *In vitro* investigations on laser lithotripsy

Ureterorenoscopic laser lithotripsy displays an important and often used method in destroying ureter stones. Still, some physical parameters are not fully understood, leading to possible operation failures. In the following, preliminary results are shown to be able to optimize the process in terms of patient- and maneuver comfort. One important aspect for the medical staff displays the fragmentation time in combination with the dusting fraction [49]. A faster fragmentation time would allow a higher efficiency in operation management as well as shorter operation times, leading to a reduction in treatment costs and stress for the patient. An improvement regarding the dusting ratio – the fraction of dust due to laser penetration over the total stone mass – is investigated. Experiments were performed, investigating the influences of different laser modes on the quantities – total fragmentation time, time before the first stone break and time afterwards chasing fragments as well as dusting to fragment ratio.

To guarantee reproducible measurement conditions, cubical stone phantoms (edge length: 5 mm) were produced. Therefore, BEGOstone Plus powder, a composition of gypsum with iron and potassium oxide [50] was mixed in the fraction 15:4 with purified water and poured into silicon forms. This choice is justified by the hardness of the resulting stone phantoms, which lies between hard urinary stones composed of calcium oxalate monohydrate and soft ones composed of magnesium ammonium phosphate hydrogen [51]. Light application was performed by a Ho:YAG laser system (AURIGA, StarMedTec, Starnberg) emitting at a wavelength of 2100 nm via a 365 μm bare fiber. The investigated laser parameters were listed in Table 1. The fragmentations were performed at the most common used laser output power of 10 W and for better comparison with half of the power [52].

Phantom stones were positioned in a water filled acrylic tube in which a central borehole (Ø: 9 mm) was drilled. Additionally five small boreholes (Ø: 2.3 mm) were added to the bottom side. These have sieve effect resulting in residual fragment sizes of < 2.3 mm that are predicted to exit the human body on the natural urinary pathways. The whole experiment was performed submerged in an aquarium set up. The laser light application fiber was inserted from above in contact with the phantom's surface.

During laser application the total time until all fragments are fallen through the sieve holes in the bottom is recorded. Additionally, the time when the stone phantom first breaks up is logged, as it displays an increase in total fragmentation time due to chasing smaller fragments. Furthermore, the amount of dust and fragment is determined afterwards. Therefore, the stones were weighed previously to the experiment. After full fragmentation, the stone fragments exited from the ureter model were selected and dried for 24 h. Afterwards again the weight was recorded. From the fraction of the two weights, the dusting ratio can be

Table 1 List of laser modes used for preliminary fragmentation efficiency measurements using 5 and 10W laser power at different pulse lengths

laser mode	pulse length/ms	energy/J	frequency/Hz	power/W
1	0.25	1.0	10	10
2	1.0			
3	1.6			
4	1.2			
5	0.25	0.5	5	5
6	0.84			
7	1.3			
8	1.6			

concluded and illustrated in mass percent. For each laser mode, five measurements were performed.

Preliminary results of the stone fragmentation with different optical pulse durations lengths are shown in Fig. 11. It showed that the ratios are almost always around 70% (dust) to 30% (fragments) except for the 0.25 ms optical pulses duration 60% (dust) and 40% (fragments). The shorter pulse lengths showed higher tendencies for early stone break time and longer total application time.

The aim of the studies was to show tendencies in improvement of laser systems by varying parameters. The results show that in principle, shorter pulses lead to a faster breakup of the stone phantom. As expected this does not lead to faster total fragmentation times, as it gets harder to chase the remaining fragments due to higher propulsion effects [53]. Hence, laser pulses with a longer optical pulse length showed later breakup times, but had shorter total fragmentation times. This theory can be supported with a look at the dusting ratios. Longer pulses show higher dusting ratios compared to shorter pulses. Combining the tendencies about breakup times, total fragmentation times and dusting ratios leads to the theory that dusting basically takes place before stone breakup.

Summarizing the gained information, longer pulses seem to be more efficient in ureterorenoscopic laser lithotripsy due to less influence of propulsion during the application. Further studies will focus on the propulsive movement of the stone phantom, adding an additional parameter to quantify the impact of the laser parameters on laser lithotripsy.

10 Conclusion

Clinically related research and development especially in biophotonics and laser medicine live from immediate

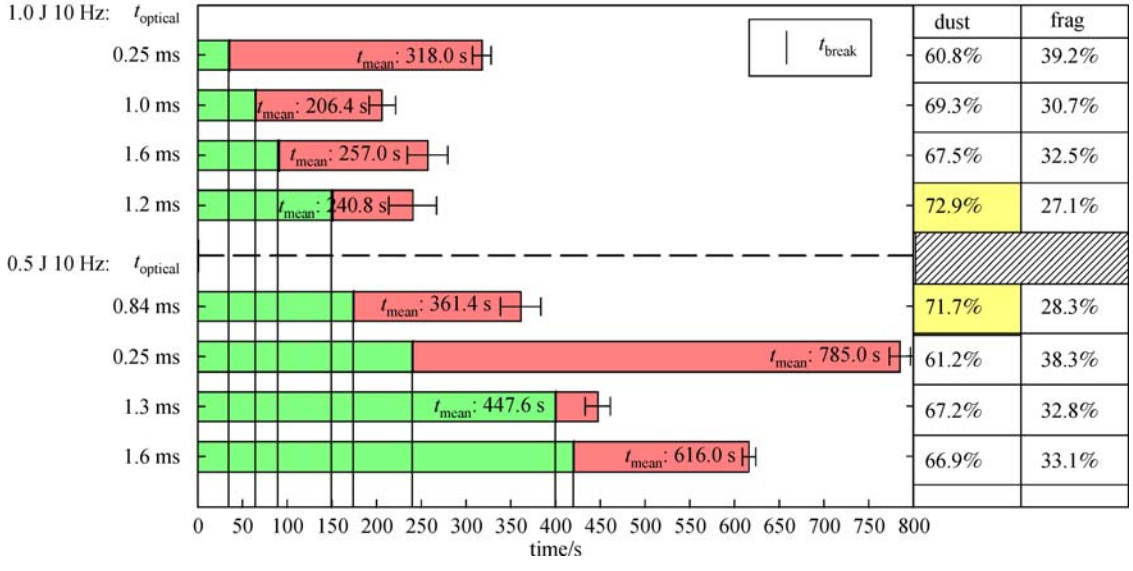

Fig. 11 Preliminary results using different optical pulse lengths, sorted by stone breaking times. The perpendicular lines illustrate the particular breaking times for each laser mode. The total fragmentation time with its standard deviation is the combination of the green bar (time before stone break) and the red bar (chasing fragments). On the right hand side the dust and fragmentation ratios are displayed in percent for each mode

communication with medical doctors thus identifying unmet needs as well as potential changes within developments. Incorporation of technicians and companies to support the development from laboratory devices to prototypes and medically approved devices to start clinical trials are indispensible. Unfortunately, even after clinical testing, sometimes in comparison to established non-optical clinical procedures, the impact, in positive or negative way, of new laser medical technologies for clinical application become obvious. This may describe the multiplicity of barriers which have to be overcome before achieving clinical acceptance [54]. The presented examples show that the knowledge about the requirements of the physicians is the basis for technical developments. The transfer of scientific knowledge into components and systems with either new or improved properties are necessary to create new innovative tools to support clinical requests. A long breath and high motivation with regard to the personal vision is needed for researches, companies and start-ups as well as for the medical doctors, also with regard to all legal hurdles, to receive clinical success for the benefit of the patients.

References

1. Labbé R F, Vreman H J, Stevenson D K. Zinc protoporphyrin: ametabolite with a mission. Clinical Chemistry, 1999, 45(12): 2060–2072
2. Hennig G, Gruber C, Vogeser M, Stepp H, Dittmar S, Sroka R, Brittenham G M. Dual-wavelength excitation for fluorescence-based quantification of zinc protoporphyrin IX and protoporphyrin IX in whole blood. Journal of Biophotonics, 2014, 7(7): 514–524
3. Hennig G, Homann C, Teksan I, Hasbargen U, Hasmüller S, Holdt L M, Khaled N, Sroka R, Stauch T, Stepp H, Vogeser M, Brittenham G M. Non-invasive detection of iron deficiency by fluorescence measurement of erythrocyte zinc protoporphyrin in the lip. Nature Communications, 2016, 7: 10776
4. Balwani M, Desnick R J. The porphyrias: advances in diagnosis and treatment. Blood, 2012, 120(23): 4496–4504
5. Enriquez de Salamanca R, Sepulveda P, Moran M J, Santos J L, Fontanellas A, Hernández A. Clinical utility of fluorometric scanning of plasma porphyrins for the diagnosis and typing of porphyrias. Clinical and Experimental Dermatology, 1993, 18(2): 128–130
6. Bonkovsky H L, Maddukuri V C, Yazici C, Anderson K E, Bissell D M, Bloomer J R, Phillips J D, Naik H, Peter I, Baillargeon G, Bossi K, Gandolfo L, Light C, Bishop D, Desnick R J. Acute porphyrias in the USA: features of 108 subjects from porphyrias consortium.The American Journal of Medicine, 2014, 127(12): 1233–1241
7. Karim Z, Lyoumi S, Nicolas G, Deybach J C, Gouya L, Puy H. Porphyrias: a 2015 update. Clinics and Research in Hepatology and Gastroenterology, 2015, 39(4): 412–425
8. Lang A, Stepp H, Homann C, Hennig G, Brittenham G M, Vogeser M. Rapid screening test for porphyria diagnosis using fluorescence spectroscopy. SPIE Proceedings, 2015, 9537: 953706
9. Rimington C. Spectral-absorption coefficients of some porphyrins in the Soret-band region. The Biochemical Journal, 1960, 75(3): 620–623
10. Westerlund J, Pudek M, Schreiber W E. A rapid and accurate spectrofluorometric method for quantification and screening of urinary porphyrins. Clinical Chemistry, 1988, 34(2): 345–351
11. Markwardt N A, Haj-Hosseini N, Hollnburger B, Stepp H, Zelenkov P, Rühm A. 405 nm versus 633 nm for protoporphyrin IX excitation in fluorescence-guided stereotactic biopsy of brain tumors. Journal of Biophotonics, 2016, 9(9): 901–912
12. Markwardt N A, Stepp H, Franz G, Sroka R, Goetz M, Zelenkov P, Rühm A. Remission spectrometry for blood vessel detection during stereotactic biopsy of brain tumors. Journal of Biophotonics, 2016
13. Gebhart S C, Lin W C, Mahadevan-Jansen A. *In vitro* determination of normal and neoplastic human brain tissue optical properties using inverse adding-doubling. Physics in Medicine and Biology, 2006, 51(8): 2011–2027
14. Yaroslavsky A N, Schulze P C, Yaroslavsky I V, Schober R, Ulrich F, Schwarzmaier H J. Optical properties of selected native and coagulated human brain tissues *in vitro* in the visible and near infrared spectral range. Physics in Medicine and Biology, 2002, 47 (12): 2059–2073
15. Johansson A, Palte G, Schnell O, Tonn J C, Herms J, Stepp H. 5-Aminolevulinic acid-induced protoporphyrin IX levels in tissue of human malignant brain tumors. Photochemistry and Photobiology, 2010, 86(6): 1373–1378
16. Prahl S A. Optical Absorption of Hemoglobin, tabulated data compiled from various sources (1999), http://omlc.ogi.edu/spectra/hemoglobin
17. Wårdell K, Hemm-Ode S, Rejmstad P, Zsigmond P. High-resolution laser Doppler measurements of microcirculation in the deep brain structures: a method for potential vessel tracking. Stereotactic and Functional Neurosurgery, 2016, 94(1): 1–9
18. Johansson A, Faber F, Kniebühler G, Stepp H, Sroka R, Egensperger R, Beyer W, Kreth F W. Protoporphyrin IX fluorescence and photobleaching during interstitial photodynamic therapy of malignant gliomas for early treatment prognosis. Lasers in Surgery and Medicine, 2013, 45(4): 225–234
19. Rühm A, Stepp H, Beyer W, Hennig G, Pongratz T, Sroka R, Schnell O, Tonn J C, Kreth F W. 5-ALA based photodynamic management of glioblastoma. Proceedings of the Society for Photo-Instrumentation Engineers, 2014, 8928: 89280E
20. Wang L V, Wu H I. Biomedical Optics: Principles and Imaging. New Jersey: Wiley, 2007
21. Beck T J, Kreth F W, Beyer W, Mehrkens J H, Obermeier A, Stepp H, Stummer W, Baumgartner R. Interstitial photodynamic therapy of nonresectable malignant glioma recurrences using 5-aminolevulinic acid induced protoporphyrin IX. Lasers in Surgery and Medicine, 2007, 39(5): 386–393
22. Castano A P, Mroz P, Hamblin M R. Photodynamic therapy and anti-tumour immunity. Nature Reviews. Cancer, 2006, 6(7): 535–545
23. Gollnick S O. Photodynamic therapy and antitumor immunity. Journal of the National Comprehensive Cancer Network: JNCCN,

2012, 10(Suppl 2): S40–S43
24. Korbelik M, Banáth J, Zhang W. Mreg activity in tumor response to photodynamic therapy and photodynamic therapy-generated cancer vaccines. Cancers (Basel), 2016, 8(10): E94
25. Korbelik M. Induction of tumor immunity by photodynamic therapy. Journal of Clinical Laser Medicine & Surgery, 1996, 14 (5): 329–334
26. Gollnick S O, Vaughan L, Henderson B W. Generation of effective antitumor vaccines using photodynamic therapy. Cancer Research, 2002, 62(6): 1604–1608
27. Korbelik M, Banáth J, Saw K M. Immunoregulatory cell depletion improves the efficacy of photodynamic therapy-generated cancer vaccines. International Journal of Molecular Sciences, 2015, 16(11): 27005–27014
28. Garg A D, Vandenberk L, Koks C, Verschuere T, Boon L, Van Gool S W, Agostinis P. Dendritic cell vaccines based on immunogenic cell death elicit danger signals and T cell-driven rejection of high-grade glioma. Science Translational Medicine, 2016, 8(328): 328ra27
29. Johansson A, Stepp H, Beck T, Beyer W, Pongratz T, Sroka R, Meinel T, Stummer W, Kreth F W, Tonn J C, Baumgartner R. ALA-mediated fluorescence- guided resection (FGR) and PDT of glioma. In: Proceedings of 12th World Congress of the International Photodynamic Association: Photodynamic Therapy: Back to the Future.2009, 7380
30. Schwartz C, Ruehm A, Tonn J C, Kreth S, Kreth F W. Interstitial photodynamic therapy of de-novo glioblastoma multiforme WHO IV:a feasibility study. In: Proceedings of 66th Annual Meeting of the Society of Neuro-Oncology. 2015, SURG-25
31. Stummer W, Beck T, Beyer W, Mehrkens J H, Obermeier A, Etminan N, Stepp H, Tonn J C, Baumgartner R, Herms J, Kreth F W. Long-sustaining response in a patient with non-resectable, distant recurrence of glioblastoma multiforme treated by interstitial photodynamic therapy using 5-ALA: case report. Journal of Neuro-Oncology, 2008, 87(1): 103–109
32. Kammerer R, Buchner A, Palluch P, Pongratz T, Oboukhovskij K, Beyer W, Johansson A, Stepp H, Baumgartner R, Zimmermann W. Induction of immune mediators in glioma and prostate cancer cells by non-lethal photodynamic therapy. PLoS One, 2011, 6(6): e21834
33. Etminan N, Peters C, Lakbir D, Bünemann E, Börger V, Sabel M C, Hänggi D, Steiger H J, Stummer W, Sorg R V. Heat-shock protein 70-dependent dendritic cell activation by 5-aminolevulinic acid-mediated photodynamic treatment of human glioblastoma spheroids in vitro. British Journal of Cancer, 2011, 105(7): 961–969
34. Navarro L, Min R J, Boné C. Endovenous laser: a new minimally invasive method of treatment for varicose veins–preliminary observations using an 810 nm diode laser. Dermatol Surgery, 2001, 27(2): 117–122
35. Min R J, Zimmet S E, Isaacs M N, Forrestal M D. Endovenous laser treatment of the incompetent greater saphenous vein. Journal of Vascular and Interventional Radiology: JVIR, 2001, 12(10): 1167–1171
36. Mordon S R, Wassmer B, Zemmouri J. Mathematical modeling of endovenous laser treatment (ELT). Biomedical Engineering Online, 2006, 5(1): 26
37. Minaev V P, Sokolov A L, Lyadov K V, Lutsenko M M, Zhilin K M. Endovenous laser treatment (EVLT) of safernous vein reflux with 1.56 μm laser. Proceedings of the Society for Photo-Instrumentation Engineers, 2009, 7373: 73731D
38. Schmedt C G, Sroka R, Steckmeier S, Meissner O A, Babaryka G, Hunger K, Ruppert V, Sadeghi-Azandaryani M, Steckmeier B M. Investigation on radiofrequency and laser (980 nm) effects after endoluminal treatment of saphenous vein insufficiency in an *ex-vivo* model. European Journal of Vascular and Endovascular Surgery, 2006, 32(3): 318–325
39. Sroka R, Weick K, Steckmaier S, Steckmaier B, Blagova R, Sroka I, Sadeghi-Azandaryani M, Maier J, Schmedt C G. The ox-foot-model for investigating endoluminal thermal treatment modalities of varicosis vein diseases. ALTEX, 2012, 29(4): 403–410
40. Sroka R, Weick K, Sadeghi-Azandaryani M, Steckmeier B, Schmedt C G. Endovenous laser therapy–application studies and latest investigations. Journal of Biophotonics, 2010, 3(5-6): 269–276
41. Sroka R, Pongratz T, Siegrist K, Burgmeier C, Barth H D, Schmedt C G. Endovenous laser application. Strategies to improve endoluminal energy application. Phlebologie, 2013, 42(3): 121–129
42. Sroka R, Schmedt C G, Steckmeier S, Meissner O A, Beyer W, Babaryka G, Steckmeier B. *Ex-vivo* investigation of endoluminal vein treatment by means of radiofrequency and laser irradiation. Medical Laser Application, 2006, 21(1): 15–22
43. Gloviczki P, Comerota A J, Dalsing M C, Eklof B G, Gillespie D L, Gloviczki M L, Lohr J M, McLafferty R B, Meissner M H, Murad M H, Padberg F T, Pappas P J, Passman M A, Raffetto J D, Vasquez M A, Wakefield T W. The care of patients with varicose veins and associated chronic venous diseases: clinical practice guidelines of the Society for Vascular Surgery and the American Venous Forum. Journal of Vascular Surgery, 2011, 53(5Suppl): 2S–48S
44. National Guideline. Varicose veins in the legs. The diagnosis and management of varicose veins. Agency for Healthcare Research and Quality (AHRQ), Rockville MD
45. Davidson S R H, Vitkin I A, Sherar M D, Whelan W M. Characterization of measurement artefacts in fluoroptic temperature sensors: implications for laser thermal therapy at 810 nm. Lasers in Surgery and Medicine, 2005, 36(4): 297–306
46. Klingenberg M, Bohris C, Niemz M H, Bille J F, Kurek R, Wallwiener D. Multifibre application in laser-induced interstitial thermotherapy under on-line MR control. Lasers in Medical Science, 2000, 15(1): 6–14
47. Grattan K T V, Selli R K, Palmer A W. Ruby fluorescence wavelength division fiber-optic temperature sensor. Review of Scientific Instruments, 1987, 58(7): 1231–1234
48. Sroka R, Hemmerich M, Pongratz T, Siegrist K, Brons J, Linden S, Meier R, Schmedt C G. Endovenous laser application. Possibilities of online monitoring. Phlebologie, 2013, 42(3): 131–138
49. Bader M J, Pongratz T, Khoder W, Stief C G, Herrmann T, Nagele U, Sroka R. Impact of pulse duration on Ho:YAG laser lithotripsy: fragmentation and dusting performance. World Journal of Urology, 2015, 33(4): 471–477
50. Simmons W N, Cocks F H, Zhong P, Preminger G. A composite kidney stone phantom with mehanical properties controllable over the range of properties of human kidney stones. Journal of the

Mechanical Behavior of Biomedical Materials, 2010, 3(1): 130–133
51. Esch E, Simmons W N, Sankin G, Cocks H F, Preminger G M, Zhong P. A simple method for fabricating artificial kidney stones of different physical properties. Urological Research, 2010, 38(4): 315–319
52. Sea J, Jonat L M, Chew B H, Qiu J, Wang B, Hoopman J, Milner T, Teichman J M. Optimal power settings for Holmium:YAG lithotripsy. The Journal of urology, 2012, 187(3): 914–919
53. Kang H W, Lee H, Teichman J M H, Oh J, Kim J, Welch A J. Dependence of calculus retropulsion on pulse duration during Ho: YAG laser lithotripsy. Lasers in Surgery and Medicine, 2006, 38(8): 762–772
54. Sroka R, Stepp H, Hennig G, Brittenham G M, Rühm A, Lilge L. Medical laser application: translation into the clinics. Journal of Biomedical Optics, 2015, 20(6): 061110

Ronald Sroka is the head of the Laser-Forschungslabor (LFL) at LIFE-Centre of University Hospital of Munich. He is mostly engaged in the research and development of fluorescence diagnosis, Photodynamic Therapy (PDT) and laser surgery in nearly all medical disciplines focusing on the translational technical implementation of several laser applications into the clinics. He is the General Secretary of the German Society of Lasermedicine (DGLM e.V.) and executive member of the ELA. Since 2015 he is adjunct professor and advisory board member of the Institute of Photomedicine Tongji-University Shanghai.

Nikolas M. Dominik (B.Sc.) received his B.Sc. (2016) degree in Physics at Ludwig-Maximilians-University Munich. Currently, he is pursuing a M.Sc. at the Laser-Foschungslabor (LFL) in LIFE-Center of University Hospital of Munich. He participates in an international research project aimed at improving stereotactic brain tumor biopsies by using fluorescence spectroscopy and remission spectrometry.

Max Eisel began his studies in applied physics at the University of Applied Sciences Munich after finishing school in 2009, and finished his Bachelor degree after completing his thesis at Truma GmbH in 2014. Afterwards he received his master degree in Photonics at the University of Applied Sciences in 2016 by finishing his master thesis at the Laser-Forschungslabor (LFL) in LIFE-Center of University Hospital of Munich. Since that time he is a PhD Student at the LFL working on investigations to improve clinical laser induced lithotripsy.

Anna Esipova is serving as medical doctor at the Department of Vascular Surgery, Diakonie Klinikum, Schwäbisch Hall, Germany. She performed clinical studies related to laser assisted endoluminal treatment of varicose vein which should aim in her medical doctoral thesis.

Christian Freymüller started studying at the University of Applied Sciences Munich after working as a Groß- und Kleinschreibung until 2011. He received his B.Eng. in Mechatronic/Precision Engineering in 2015 working at the Institute of Atmospheric Physics, German Aerospace Center (DLR). Subsequently, he started his Master degree in Photonics at the University of Applied Sciences Munich. In this context he is currently writing his master thesis focusing on the application of thermography for medical application at Laser-Forschungslabor (LFL) in LIFE-Center of University Hospital University, Ludwig-Maximilians University Munich.

Christian Heckl received his Bachelor degree from the University for Applied Science in Regensburg, Germany, working on the characterization of silicon field emitters as an electron source for a miniaturized X-ray source. In 2015 he started a Master studies in Photonics at the University for Applied Science in Munich and performed Master degree at the Laser-Forschungslabor (LFL) in LIFE-Center of the University Hospital of Munich investigating screening tests for laboratory medicine using fluorescence spectroscopy.

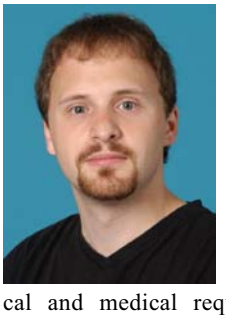

Georg Hennig holds his Ph.D. degree from the Medical Faculty of the LMU Munich and is senior researcher in Laser-Forschungslabor (LFL) in LIFE-Center of University Hospital of Munich. He focuses on experimental quantification of fluorescence light from tissue as well as Monte Carlo modeling of light propagation. His deep understanding of both the technological and medical requirements supports the development of innovative medical diagnostic devices.

Christian Homann (Ph.D.) received his Diploma in Physics in 2006 from the Ludwig-Maximilians-Universität in Munich. In 2013 he obtained his doctor's degree with works in the field of non-linear optics. Since then he is located at the Laser-Forschungslabor (LFL) at LIFE-Center of the University Hospital of Munich. His main research focus is on medical applications of lasers and spectroscopy, especially on fluorescence detection in tissues.

Nicolas Hoehne is part of a spin-off project at the Laser Forschungslabor (LFL) in LIFE-center of the University Hospital of Munich. The project aims to found a start-up company and to market a non-invasive point-of-care testing device that detects the iron parameter Zinc-Protoporphyrin. He has been responsible for Finance, Controlling and Project Management. He is a chartered Global Management Accountant and holds a M.Sc. degree in Controlling from the UCD Michael Smurfit Graduate School Dublin.

Robert Kammerer received his Ph.D. degree as veterinarian at University Gießen Germany in 1993 and performed his habilitation thesis at the Medical Faculty of the University Munich. Today he is specialist in immunology and serology in veterinary medicine at Institute for Immunology of the Friedrich-Löffler-Institute which is a Federal Research Institute for Animal Health in Rostock, Germany.

Thomas Kellerer studies Physical Engineering at the University of Applied Science in Munich graduating as Bachelor of Science in 2018. At the Laser-Forschungslabor (LFL) in LIFE Center of University Hospital Munich, he is involved in testing and improvement of specified laser-spectroscopy devices.

Alexander Lang began his studies in Physics at Technical University Munich (TUM), where he finished with a Bachelor (B.Sc.) and a Master Degree in Physics of Condensed Matter in 2015. During his bachelor thesis, he was involved in the construction of an optical setup for the generation of bicolored femtosecond pulses using second harmonic generation at the Max-Planck-Institute for Quantum Optics in Garching. During his master thesis, he started working towards a screening test for the quantifications of porphyrins in blood plasma and translated this into his current project of his PhD-thesis, which aims at developing a test method for acute porphyria.

Niklas A. Markwardt (M.Sc.) received his B.Sc. (2011) and M.Sc. (2013) degrees in Physics at Ludwig-Maximilians-University Munich, focusing his studies on astrophysics and biophysics. Currently, he is pursuing a PhD at the Laser-Forschungslabor (LFL) in LIFE-Center of the University Hospital of Munich. His main research focus lies on fluorescence diagnosis and photodynamic therapy. He participates in a joint research project aimed at improving stereotactic brain tumor biopsies by using fluorescence spectroscopy.

Thomas Pongratz (Dipl.-Ing. FH) serves as a development engineer at the Laser-Forschungslabor (LFL) in LIFE Center at the university Hospital of Munich after studying at the University of Applied Sciences Munich. He is mainly involved in the development, testing and validating of light-application systems for photodynamic therapy and diagnosis, investigating and designing of light dosimetry concepts and laser lithotripsy. Furthermore he serves as technical assistance in the operating room during laser treatments.

Claus-Georg Schmedt is the Head of the Department of Vascular Surgery, Diakonie Klinikum, Schwäbisch Hall, Germany since 2010. Since 2004 he is involved in the development of innovative treatment techniques for varicose vein disease. As a surgeon he performed a variety of preclinical experiments to improve and compare different laser assisted approaches. Furthermore, he is the organiser of specific training courses in this field.

Dr. rer. biol. hum. **Herbert Stepp** is Physicist (Technical University of Munich) with a dissertation at the Medical Faculty of the Ludwig-Maximilians-University in Munich. He his research group leader at the Laser-Forschungslabor (LFL) in LIFE-Centre of the University Hospital of Munich. His scientific focus is on biophotonics for clinical applications with achievements in fluorescence guided surgery, photodynamic therapy and non-invasive detection of iron deficiency.

Stephan Ströbl began his studies in Physics at the LMU, Munich after finishing school in 2012. In 2015 he finished his Bachelor degrees after completing his work for the Bachelor thesis at the Laser-Forschungslabor (LFL) of the LIFE-Centre at the University Hospital of Munich. During his Bachelor studies he spent one term at the University of Auckland, New Zealand, studying Physics. During his Bachelor and the following Master degree, his scientific focus is on medical physics. Since 2016 he returned to the LFL to perform his master thesis on laser-induced Ho:YAG Lithotripsy.

Prof. Dr. rer. nat. **Wolfgang Zimmermann** studied chemistry (University of Würzburg, Germany) and obtained his doctoral degree at the Department of Chemistry and Biochemistry of the Ludwig-Maximilians-University in Munich. In 1999 he cofounded the biotech company Genovac/Aldevron in Freiburg, Germany which develops antibodies for research and therapy by genetic immunization. Before his recent retirement he was managing director of the LIFE Center and the Tumor Immunology Laboratory at the University Hospital of Munich. His scientific interests encompass tumor immunology and biology, cancer stem cells and evolution of the carcinoembryonic antigen gene family.

Dr. **Adrian Rühm** obtained his Physics Diploma at the LMU in Munich in 1993. He holds a Ph.D. degree in Physics and has been working in the fields of Physics and Materials Science for the Max Planck Institute for Metals Research in Stuttgart, for the Massachusetts Institute of Technology, Boston, at the Advanced Photon Source at Argonne National Laboratory, and at the Research Neutron Source in Garching near Munich. In 2011 he joined the Laser-Forschungslabor (LFL) at the LIFE Center of the University Hospital of the LMU in Munich. He is working as a senior scientist in the field of biomedical optics and medical laser applications, with a focus on interstitial photodynamic therapy (iPDT) and fluorescence lifetime imaging (FLIM).